ARTICLE

Ordered Mesoporous Polymer−Silica Hybrid Nanoparticles as Vehicles for the Intracellular Controlled Release of Macromolecules

Tae-Wan Kim,[†,*] Igor I. Slowing,[‡] Po-Wen Chung,[‡] and Victor Shang-Yi Lin[‡]

[†]Green Chemistry Research Division, Korea Research Institute of Chemical Technology, P.O. Box 107, Sinseongro 19, Yuseong-gu, Daejeon 305-600, Korea, and [‡]Department of Chemistry, U.S. Department of Energy Ames Laboratory, Iowa State University, Ames, Iowa 50011-3111, United States

ABSTRACT A two-dimensional hexagonal ordered mesoporous polymer−silica hybrid nanoparticle (PSN) material was synthesized by polymerization of acrylate monomers on the surface of SBA-15 mesoporous silica nanoparticles. The structure of the PSN material was analyzed using a series of different techniques, including transmission electron microscopy, powder X-ray diffraction, and N_2 sorption analysis. These structurally ordered mesoporous polymer−silica hybrid nanoparticles were used for the controlled release of membrane-impermeable macromolecules inside eukaryotic cells. The cellular uptake efficiency and biocompatibility of PSN with human cervical cancer cells (HeLa) were investigated. Our results show that the inhibitory concentration (IC_{50}) of PSN is very high (>100 μg/mL per million cells), while the median effective concentration for the uptake (EC_{50}) of PSN is low (EC_{50} = 4.4 μg/mL), indicating that PSNs are fairly biocompatible and easily up-taken *in vitro*. A membrane-impermeable macromolecule, 40 kDa FITC-Dextran, was loaded into the mesopores of PSNs at low pH. We demonstrated that the PSN material could indeed serve as a transmembrane carrier for the controlled release of FITC-Dextran at the pH level inside live HeLa cells. We believe that further developments of this PSN material will lead to a new generation of nanodevices for intracellular controlled delivery applications.

KEYWORDS: mesoporous polymer−silica composite · endocytosis · cellular uptake · drug delivery · mesostructured nanoparticles · controlled release

*Address correspondence to twkim@krict.re.kr.

Received for review July 1, 2010 and accepted December 2, 2010.

Published online December 16, 2010. 10.1021/nn101740e

Large-pore ordered mesoporous silica (OMS) materials were first synthesized by Stucky and co-workers using poly(ethylene oxide)-poly(propylene oxide)-poly(ethyleneoxide)-type nonionic triblock copolymers as templates.[1] The uniform pores of these OMS materials are typically larger than 5 nm in diameter—this has enabled their successful application in a variety of processes that involve large molecules, such as the adsorption and separation of bulky species, the immobilization of enzymes, and the catalytic transformation of macromolecules.[1−8] One of the limitations of these materials is that they cannot be applied to some processes such as intracellular drug delivery that require a well-defined particle morphology and a monodisperse submicrometer particle size.[9] Typically, SBA-15 OMS materials have micrometer size rod-like shapes or are amorphous polydisperse powders with a rather long pore axis length as compared to monodispersed spherical MCM-41 mesoporous silica nanoparticles (MSN) obtained with cationic surfactants as structural directing agents.[5,10−13] Furthermore, OMS materials tend to aggregate in suspension, which limits their uptake by living cells and thus prevents their use as intracellular delivery agents for macromolecules. There have been few reports on the synthesis of submicrometer size SBA-15, and the particle shape is still not clearly defined, with large aggregates being formed in most cases.[11,14−17]

The other important issue regarding the prospect of using OMS for biomedical applications, such as controlled drug release, is functionalization of the surface of the material. Organo-functionalized mesoporous materials have been considered for applications in diverse fields such as heterogeneous catalysis, separation, membrane technologies, sensors, drug delivery, and nanomedicine.[2−4,6,7,11,13,18−23] Extensive efforts toward the functionalization of OMS have been exerted using different approaches, such as postsynthesis grafting, co-condensation, and postpolymerization.[2,12,13,18,22,24,25] In the postpolymerization method, mesoporous polymer−inorganic hybrid materials are synthesized using *in situ* free-radical polymerization of vinyl-based monomers confined at the mesopore surface.[24,26−28] After polymerization of the monomers, a thin layer of polymer is formed on the surface of the OMS, while the mesopores remain fully accessible. This method makes it possible to

exploit the desired physical properties of the OMS, for example, large pore diameter, ordered mesostructure, given particle shape/size, for the preparation of specific functional organic−inorganic hybrid mesoporous materials. In addition, a large variety of surface functional groups are available through this approach, as they can be controlled by the addition of different functional monomers and the polymerization conditions.

In this study, we report a method to synthesize organic−inorganic hybrid nanoparticles based on the structural features of SBA-15 nanoparticles. The resulting polymer−mesoporous silica hybrid nanoparticle (PSN) materials possess a morphology that is suitable for cellular uptake, display high biocompatibility, and are capable of controlled intracellular delivery of macromolecular species. In addition, PSNs are highly monodispersed, have a particle size of 500−600 nm, and preserve the 2-D hexagonal structure of the original SBA-15 nanoparticles. These PSNs are prepared by combining a recently developed postpolymerization method for surface functionalization with a technique for controlling the growth and morphology of SBA-15.[24,29] As detailed below, we have confirmed that the fabricated PSNs are biocompatible and could be efficiently endocytosed by human cervical cancer cells (HeLa). Furthermore, our experimental data indicated that these PSN materials could serve as intracellular delivery vehicles for the pH-dependent controlled release of a cell membrane-impermeable macromolecule, 40 kDa FITC-Dextran (Scheme 1). This study represents a first step toward the biomedical application of nanosized large pore SBA-15-like materials, demonstrating adequate biocompatibility, easy endocytosis, and controlled release of macromolecules.

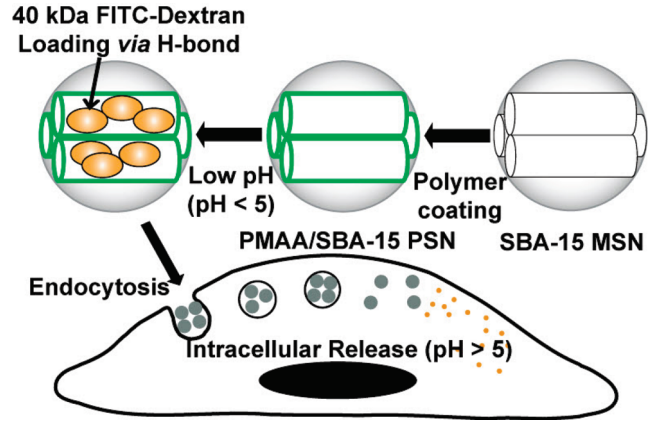

Scheme 1. Schematic representation of the endocytosis and intracellular controlled release delivery of PSN materials.

RESULTS AND DISCUSSION

Ordered mesoporous polymer−silica hybrid nanoparticles (PSNs) were successfully synthesized by following a two-step synthesis. First, we synthesized SBA-15-type mesoporous silica nanoparticles (MSNs) by modifying a method previously reported in the literature.[29] SBA-15-type MSNs with a mean diameter of about 500−600 nm were prepared using a triblock copolymer Pluronic P104 as a structure-directing agent and tetramethyl orthosilicate (TMOS) as a silica precursor. The final hybrid PSN materials were obtained by *in situ* free-radical polymerization of vinyl-based monomers and cross-linkers *via* a process initially developed by Ryoo *et al.*[24] As described in the Experimental Section, methacrylic acid (MAA) monomer, ethylene dimethacrylate (EDMA) cross-linker, and a dichloromethane solution of azobisisobutyronitrile (AIBN) radical initiator were introduced into the mesopores of calcined SBA-15 MSNs *via* incipient wetness, followed by a radical-triggered polymerization under vacuum.

The structure of the PSN was analyzed using a series of different techniques, including transmission electron microscopy (TEM), powder X-ray diffraction (XRD), and N_2 sorption analysis. As depicted in Figure 1a, the PSNs consisted of monodisperse (500−600 nm) truncated spherical nanoparticles. Compared to SBA-15 MSNs, depicted in Figure S1 (Supporting Information),

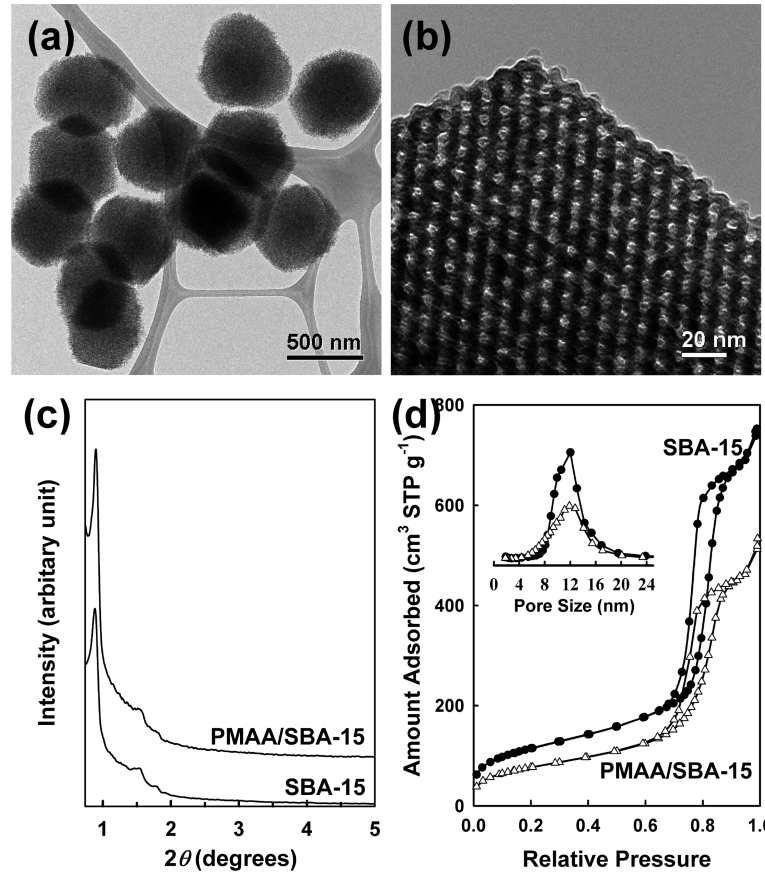

Figure 1. (a) Low- and (b) high-magnification TEM images of PMAA-coated mesoporous polymer−silica hybrid nanoparticle (PMAA/SBA-15 PSN) materials. (c) Powder XRD patterns of PMAA/SBA-15 PSN (top) and the calcined SBA-15 MSN (bottom). (d) N_2 sorption isotherm and the pore size analysis with an adsorption branch using the BJH algorithm (inset) of SBA-15 MSN and PMAA/SBA-15 PSN.

TABLE 1. Structural Properties of SBA-15 Mesoporous Silica Nanoparticles and Ordered Mesoporous Polymer−Silica Hybrid Nanoparticle PMAA/SBA-15 PSN from Nitrogen Adsorption Data[a] and Hydrodynamic Particle Size and ζ-Potential from a Particle Analyzer

sample	S_{BET} [$m^2 g^{-1}$]	V_t [$cm^3 g^{-1}$]	w_{BHJ} [nm]	particle size[b] [nm]	ζ-potential [mV]
SBA-15	419	1.07	12.0	531 ± 0.0	−26.6 ± 1.280
PMAA/SBA-15	283	0.71	11.7	587 ± 40	−27.3 ± 0.703

[a] S_{BET} is the BET specific surface area calculated in the range of relative pressures from 0.05 to 0.2; V_t is the total pore volume calculated at the relative pressure of about 0.95; w_{BJH} is the diameter of mesopores calculated using the BJH method. [b] Hydrodynamic particle size from dynamic light scattering (DLS) measurements.

the TEM micrograph of the PSNs indicates preservation of the particle morphology and particle size. It can be observed in Figure 1b that the PSNs maintain highly ordered mesoporous structures with a two-dimensional (2-D) hexagonal *p6mm* symmetry after incorporation of a thin layer of cross-linked poly(methacrylic acid) (PMAA) on the silica surface. Powder XRD patterns of SBA-15 MSNs and PSNs show highly ordered 2-D hexagonal mesostructures (Figure 1c). The increasing (100) XRD peak intensity of the PSN sample is due to the uniform coating of polymer on the surface of the SBA-15 MSN mesopores. This leads to a relative increase of the density of the mesopore walls, which in turn results in increased X-ray scattering contrast.[24] The thermogravimetric analysis (TGA) results presented in Figure S2 (Supporting Information) indicate that 78% of the monomers were polymerized. Nitrogen adsorption−desorption measurements at −196 °C (Figure 1d) show typical type IV isotherms for all of the samples, with sharp capillary condensation steps at high relative pressure (P/P_0 = 0.7−0.9) and H1 hysteresis loops, indicative of well-defined cylindrical pores. After polymer deposition on the surface of the SBA-15 MSNs, the porosity values of the PSN are reduced compared to the parent SBA-15 MSNs, but the PSNs retain a large BET specific surface area (283 m^2/g), a high pore volume (0.71 cm^3/g), and a comparable pore diameter (11.7 nm) (Table 1). Dynamic light scattering (DLS) and ζ-potential measurement were performed to observe any differences between the original SBA-15 MSNs and the PMAA-coated PSNs. From these investigations, it was found that the values of hydrodynamic particle size and ζ-potential PSN remained similar to those of the original SBA-15 MSNs. This suggests that most of the monomers are indeed polymerized inside the mesopores of SBA-15 MSN and do not aggregate outside the pores during the polymerization process. Furthermore, the PSNs remain isolated with no interparticle aggregation due to external polymer cross-linking.

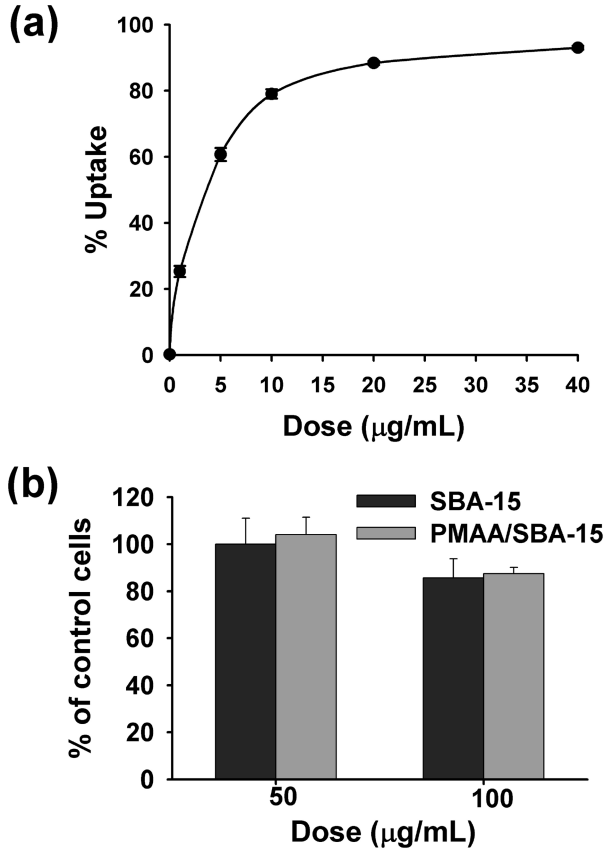

Figure 2. (a) Uptake of the PMAA/SBA-15 PSNs by HeLa cells as a function of concentration. (b) Viability test of HeLa cells with different concentrations of SBA-15 and PSN after 48 h incubation.

To investigate the cell membrane permeability of PSNs, we incubated human cervical cancer cells (HeLa) in suspensions of fluorescein-labeled PSN (1−40 μg/mL) in Dubelcco's Eagle Modified Medium (DMEM). After 10 h incubation at 37 °C in a CO_2 atmosphere, the cells were washed, harvested by trypsinization, and resuspended in trypan blue quencher for analysis by flow cytometry (for further details, see the Supporting Information). As can be noted in Figure 2a, the uptake of the material by the cells was highly efficient, with an EC_{50} value of 4.4 μg/mL. The biocompatibility of SBA-15 MSNs and PSNs was evaluated by incubating HeLa cells with MSN and PSN suspensions of different concentrations (50 and 100 μg/mL) in growth media for 48 h. After washing and harvesting, the cell viability and proliferation were analyzed using a GuavaViacount cytometry assay, as detailed in the Supporting Information. No growth inhibition was found at concentrations as high as 50 μg/mL. As shown in Figure 2b, the high inhibitory concentration (IC_{50} > 100 μg/mL per million cells) indicated that both SBA-15 MSNs and PSNs are very biocompatible *in vitro*.

To investigate the efficacy of PSNs as an intracellular carrier for macromolecules, a cell membrane-impermeable macromolecule, 40 kDa FITC-Dextran, was loaded into PSNs. The estimated hydrodynamic diameter of 40 kDa FITC-Dextran is approximately 8 nm.[30] This is still smaller than the pore diameter of PMAA/SBA-15 PSN (11.7 nm), which is thus sufficient to permit diffusion of 40 kDa FITC-Dextran molecules inside the mesopores of PSNs.[31,32] As shown in Figure 3a, the

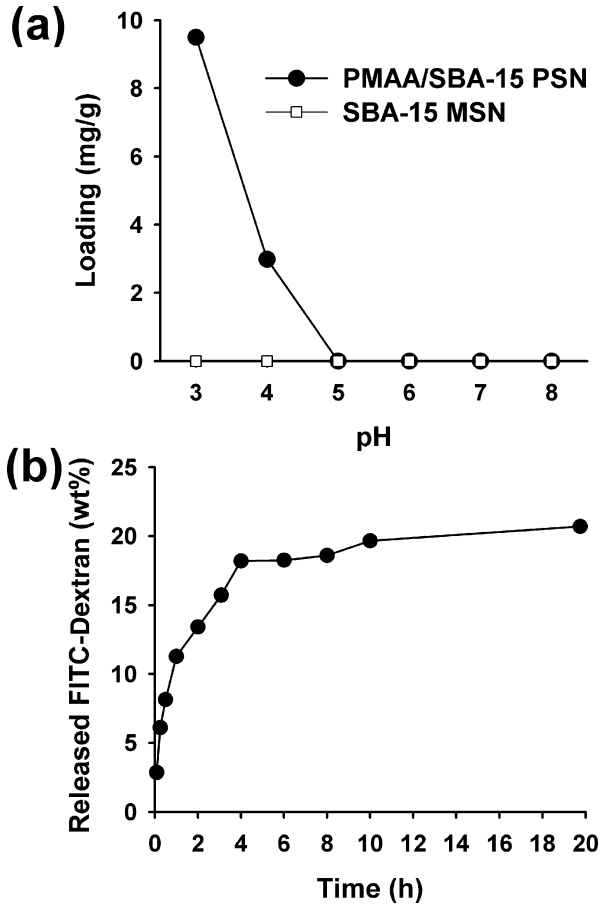

Figure 3. (a) The pH-dependent adsorption profile of 40 kDa FITC-Dextran to PMAA/SBA-15 PSN and SBA-15 MSN, and (b) release profile of FITC-Dextran from PSNs in pH 7 PBS solution at room temperature. FITC-Dextran was loaded to the PSN sample at pH 3.

adsorption ability of the PSN material for FITC-Dextran was dependent on the pH of the loading suspension. Low pH solutions (pH $<$ 5) lead to high loading of FITC-Dextran into the PSNs. This could be caused by the formation of stabilized complexes between the carboxylic acid groups of PMAA and hydroxyl groups of dextran *via* hydrogen bonding.[33] In contrast, at pH higher than 5, FITC-Dextran could not be loaded into PSNs. The existing literature reports a pK_a value of 4.85 for PMAA.[34] Consequently, hydrogen-bonded complexes would not be favored, because of deprotonation of the carboxylic acid groups of PMAA. It is well-known that dextran typically has poor affinity to solid surfaces.[35] These results demonstrate that the carboxylic acid moieties on the surface provide a mechanism to control the loading and release of dextran from the mesopores of PSNs by simply varying the pH of the suspension.

In order to further study the controlled release of FITC-Dextran as a function of pH, we prepared a FITC-Dextran-loaded PSN sample at pH 3 and analyzed the release profile in pH 7 PBS solution. As shown in Figure 3b, 40 kDa FITC-Dextran could indeed be released efficiently from the PSNs in the pH 7 PBS solution. A rapid release of 16 wt % of the loaded FITC-Dextran was observed within the first 4 h at pH 7, and the rate of release thereafter diminished, reaching only 21 wt % after 20 h. These results support the hypothesis that adsorption and release of FITC-Dextran are governed by pH.

To investigate the intracellular controlled release, FITC-Dextran-loaded PSN (9.5 mg/g) and free FITC-Dextrans were suspended in cell growth media at the same concentration as the macromolecule (10 μg/mL for the composite and 95 ng/mL for the free macromolecules). The suspensions were then added to HeLa cells grown under glass coverslips and incubated for 12 h at 37 °C in a 5% CO_2 atmosphere. The

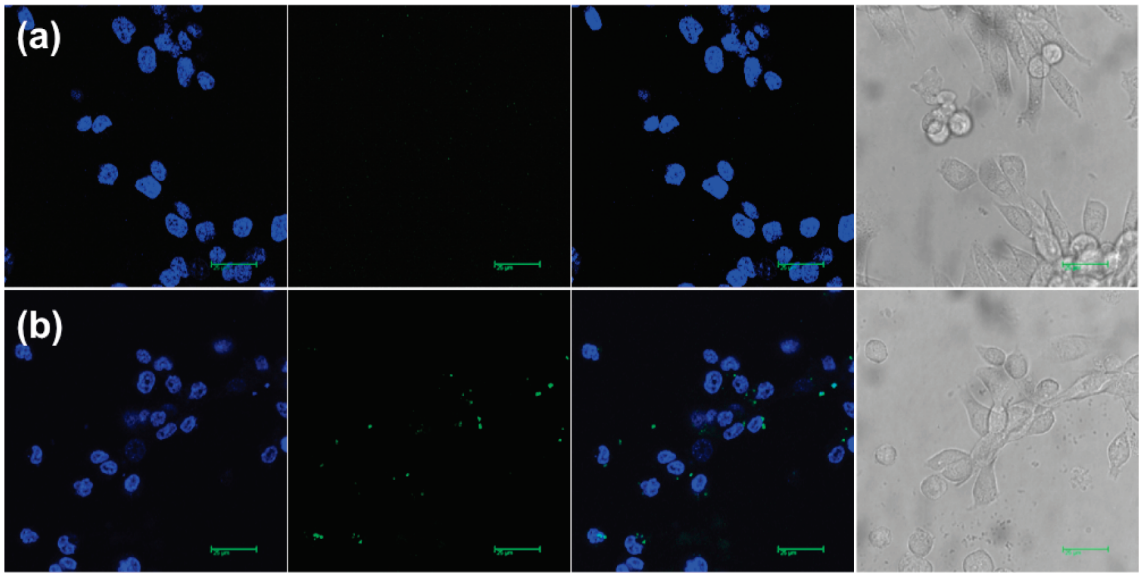

Figure 4. Confocal fluorescence micrographs of HeLa cells with (a) free FITC-Dextran and (b) FITC-Dextran-loaded PMAA/SBA-15 PSN. The images from left to right correspond to stained cell nuclei (blue), FITC-Dextran (green), merging of both, and the phase contrast image. The scale bar is 25 μm. The presence of green fluorescence at the same focal plane as the nuclei and at the same location as the cell bodies demonstrates that the cells internalized the FITC-Dextran-loaded particles.

cells were subsequently stained with nuclear dye Hoechst 33258 and lipophilic dye FM 4-64. The slips containing the cells were then washed with PBS and transferred to microscope slides with 15 μL of fresh growth media for immediate observation under a confocal fluorescent microscope. As seen in Figure 4a, the confocal micrographs show that due to its large molecular size the 40 kDa FITC-Dextran was not internalized by the HeLa cells in the absence of PSNs. No FITC fluorescence was observed inside of the cell bodies. In contrast, in the presence of PSNs, an intense green fluorescence was visible in the same focal plane as the cell nuclei, as shown in the confocal fluorescence image (Figure 4b). This observation clearly indicated that 40 kDa FITC-Dextran macromolecules were indeed delivered through the cell membrane of HeLa by PSN.

In conclusion, we have demonstrated that polymer−mesoporous silica hybrid nanoparticle materials can be efficiently internalized by HeLa cells with low cytotoxicity. In addition, it was shown that the PSN material can indeed serve as a transmembrane carrier for the controlled release of macromolecules inside living HeLa cells. We believe that this PSN material will lead to a new generation of nanodevices for intracellular controlled delivery of bioactive macromolecules.

EXPERIMENTAL SECTION

Materials. ***Preparation of SBA-15 MSNs.*** A triblock copolymer (Pluronic P104, $EO_{27}PO_{61}EO_{27}$; 7.0 g) was fully dissolved in 273.4 g of a 1.6 M HCl aqueous solution at 56 °C. Tetramethyl orthosilicate (TMOS; 10.6 g) was quickly added into the solution at 56 °C. After continuous stirring for 24 h, the reaction mixture was moved to a Teflon-lined high-pressure autoclave for further hydrothermal treatment at 150 °C for 24 h. After hydrothermal treatment, the resulting solid SBA-15-type MSN product was isolated by filtration, washed with copious amounts of water and methanol, and air-dried at 80 °C. Template-free MSN was obtained through a high-temperature calcination process at 550 °C.

Preparation of PSNs. To synthesize mesoporous polymer−silica hybrid nanoparticle (PSN), methacrylic acid (MAA; 0.190 g) monomer, ethylene dimethacrylate (EDMA; 0.110 g) cross-linker, and a,a-azoisobutyronitrile (AIBN; 0.0164 g) radical initiator were fully dissolved in 1.25 mL of dichloromethane. The solution was introduced into mesopores of the calcined SBA-15 MSN (1 g) *via* the impregnation method. After drying at 40 °C in a mechanical convection oven for 2 h to remove the solvent dichloromethane, the mixture was moved into a Schlenk reactor and subjected to freeze−vacuum−thaw cycles three times using liquid N_2. The mixture was kept under a vacuum condition at 35 °C for 6 h, and polymerization was performed at 60 °C for 6 h, 100 °C for 1 h, and 120 °C for 1 h. After being cooled to room temperature, the sample was washed with chloroform and ethanol and was dried at 80 °C under a vacuum.

Measurement of SBA-15 MSN and PSN. XRD patterns were recorded on a Scintag XDS-2000 instrument operated at 1.21 kW using Cu Kα radiation. Thermogravimetric analysis (TGA) of the PSN sample was performed on a TA Instruments thermal analysis system with a heating rate of 5 °C under an air flow. The nitrogen adsorption isotherms were measured at the liquid nitrogen temperature (−196 °C) using a Micromeritics ASAP2000 volumetric adsorption analyzer. The Brunauer−Emmett−Teller (BET) equation was used to calculate the apparent surface area from adsorption data obtained at P/P_0 between 0.05 and 0.2. The total volume of micro- and mesopores was calculated from the amount of nitrogen adsorbed at $P/P_0 = 0.95$, assuming that adsorption on the external surface was negligible compared to adsorption in pores. The pore size distributions (PSDs) were calculated by analyzing the adsorption branch of the N_2 sorption isotherm using the Barret−Joyner−Halenda (BJH) method. TEM images were taken on a copper grid supported with carbon film, using a Tecnai G2 F20 device operated at 200 kV. Dynamic light scattering (DLS) and ζ-potentials of SBA-15 MSN and PSN were measured on a Malvern Zetasizer-Nano instrument equipped with a 4 mW He−Ne laser (632.8 nm) and an avalanche photodiode detector. Suspensions (200 μg/mL) of each material in PBS buffer were prepared. The DLS and ζ-potential were measured immediately after ultrasonication for 15 min.

Cellular Uptake. ***Fluorescent Labeling of Polymer−Mesoporous Silica Nanoparticles (PSNs).*** Anhydrous potassium carbonate (16.1 mg, 116 μmol), 18-crown-6 (9.0 mg, 33 μmol), and 5-bromomethylfluorescein (2.1 mg, 4.7 μmol) were suspended in 0.3 mL of anhydrous acetonitrile. The mixture was added to a suspension of 16.1 mg of PSN in 1.0 mL of anhydrous acetonitrile and was stirred at 60 °C under protection from light for 4 h. The product was recovered by centrifugation and washed several times with methanol and water.

Flow Cytometry. HeLa cells were seeded in 6-well plates at a concentration of 1 × 105 cells/mL (3 mL per well) in D-10 growth medium, consisting of Dubbelco's Modified Eagle Medium (DMEM) supplemented with equine serum (10%), penicillin, streptomycin, gentamicin, and alanylglutamine. The cells were then incubated for 30 h at 37 °C in a 5% CO_2 atmosphere. The media were then removed from the wells, and the attached cells were washed with phosphate buffered saline (PBS). The wells were subsequently filled with suspensions of fluorescein-labeled PSN in serum-free growth media at various concentrations. The plates were then set back into the incubator for an additional 10 h. After the incubation period, the supernatant was removed and the cells were washed with PBS and harvested by trypsinization. After centrifugation, the cell pellets were resuspended in trypan blue solution and analyzed by fluorescence-activated cell sorting (FACS) in a Becton-Dickinson FACS Canto flow cytometer. Each concentration was tested in triplicate.

Fluorescence Confocal Imaging. HeLa cells were seeded at a concentration of 0.75 × 105 cells/mL in D-10 growth medium in 6-well plates containing glass coverslips. The cells were then incubated for 30 h at 37 °C in a 5% CO_2 atmosphere. The media were removed from the wells, and the attached cells were washed with phosphate buffered saline (PBS). One well then was filled with 3 mL of a 95 ng/mL suspension of FITC-Dextran in growth media, and another well was filled with 3 mL of a 10 μg/mL suspension of FITC-Dextran-loaded PMAA/SBA-15 PSN (loading: 9.5 mg of FITC-dextran/g of PMAA/SBA-15 PSN). The cells were then set back in the incubator for an additional 10 h. After this incubation period, 5 μg of lipophilic dye FM 4-64 and 50 μL of the nuclear stain Hoechst 33258 (0.5 mg/mL) were added to the wells, which were placed in the incubator for 15 more minutes. The supernatant was then removed, and the coverslips with the attached cells were washed with PBS and transferred to microscope slides with 15 μL of fresh growth media. The slides were imaged with a 100× oil immersion objective in a Leica TCS NT laser confocal microscope at wavelengths corresponding to the nuclear stain, FITC label, and FM 4-64 lipophilic dye (excitation = 350 and 488 nm, emission = BP 455/20, BP 525/20, and LP 590, respectively).

Biocompatibility Assay. HeLa cells were seeded in 6-well plates at a concentration of 1 × 105 cells/mL (3 mL per well) in D-10 growth medium, consisting of Dubbelco's Modified Eagle Medium (DMEM) supplemented with equine serum (10%), penicillin, streptomycin, gentamicin, and alanylglutamine. The cells were incubated for 30 h at 37 °C in a 5% CO_2 atmosphere. The media were subsequently removed from the wells, and the attached cells were washed with phosphate buffered saline (PBS) and the wells filled with suspensions of the materials in D-10

growth medium at various concentrations. The plates were then placed back into the incubator for an additional 48 h. After this period, the supernatant was removed and the cells were washed with PBS and harvested by trypsinization. After centrifugation, the cell pellets were resuspended in 1.0 mL of growth medium, and 10 μL of cell suspension was mixed with 190 μL of Guava Via Count reagent (Guava Technologies, Inc., Hayward, CA); the resultant solution was left to rest 5 min. The amount of viable cells in each sample was thereafter measured by flow cytometry using a Guava Technologies Personal Cell Analyzer. Each material and concentration was tested by triplicate.

FITC-Dextran Adsorption and Release Test. FITC-Dextran (40 kDa) was dissolved in each buffer solution with different pH (pH 3−8), and 9 μM of FITC-Dextran solution was prepared. PSN (3.2 mg) was added to 5 mL of the FITC-Dextran solution in a 14 mL centrifuge tube. After the mixture was stirred for 24 h in a dark area, the final mixture was then centrifuged and washed with a buffer solution three times. The amount of FITC-Dextran loaded on the PSN was determined by analyzing the supernatant solution spectrophotometrically at 451 nm on a HP-8453 UV−vis spectrophotometer. The sample was dried under vacuum overnight at room temperature.

The release profile of 40 kDa FITC-Dextran from the PSN in pH 7 PBS solution was obtained at room temperature using the FITC-Dextran-loaded PSN at pH 3. The FITC-Dextran/PSN in PBS solution was centrifuged for a predetermined time, and the supernatant was collected. The concentration and amount of FITC-Dextran in PBS solution were determined using a fluorometer (FluoroMax-2, Instruments S.A., Inc.).

Acknowledgment. This study was supported by the U.S. DOE Ames Laboratory through the office of Basic Energy Sciences under Contract No. DE-AC02-07CH11358. The authors also thank BASF Co. for the donation of P104 triblock copolymer. We dedicate this work in memory of our esteemed colleague, Victor S.Y. Lin, deceased May 4, 2010.

Supporting Information Available: TEM images of SBA-15 nanoparticles and TGA profile of PSN. This material is available free of charge *via* the Internet at http://pubs.acs.org.

REFERENCES AND NOTES

1. Zhao, D.; Feng, J.; Huo, Q.; Melosh, N.; Fredrickson, G. H.; Chmelka, B. F.; Stucky, G. D. Triblock Copolymer Syntheses of Mesoporous Silica with Periodic 50 to 300 Angstrom Pores. *Science* **1998**, *279*, 548–552.
2. Stein, A. Advances in Microporous and Mesoporous Solids-Highlights of Recent Progress. *Adv. Mater.* **2003**, *15*, 763–775.
3. Hartmann, M. Ordered Mesoporous Materials for Bioadsorption and Biocatalysis. *Chem. Mater.* **2005**, *17*, 4577–4593.
4. Giraldo, L. F.; López, B. L.; Pérez, L.; Urrego, S.; Sierra, L.; Mesa, M. Mesoporous Silica Applications. *Macromol. Symp.* **2007**, *258*, 129–141.
5. Wan, Y.; Zhao, D. Y. On the Controllable Soft-Templating Approach to Mesoporous Silicates. *Chem. Rev.* **2007**, *107*, 2821–2860.
6. Wan, H.; Liu, L.; Li, C.; Xue, X.; Liang, X. Facile Synthesis of Mesoporous SBA-15 Silica Spheres and Its Application for High-Performance Liquid Chromatography. *J. Colloid Interface Sci.* **2009**, *337*, 420–426.
7. Moreno, J.; Sherrington, D. C. Well-Defined Mesostructured Organic−Inorganic Hybrid Materials *via* Atom Transfer Radical Grafting of Oligomethacrylates onto SBA-15 Pore Surfaces. *Chem. Mater.* **2008**, *20*, 4468–4474.
8. Kruk, M.; Dufour, B.; Celer, E. B.; Kowalewski, T.; Jaroniec, M.; Matyjaszewski, K. Grafting Monodisperse Polymer Chains from Concave Surfaces of Ordered Mesoporous Silicas. *Macromolecules* **2008**, *41*, 8584–8591.
9. Rejman, J.; Oberle, V.; Zuhorn, I. S.; Hoekstra, D. Size-Dependent Internalization of Particles *via* the Pathways of Clathrin- and Caveolae-Mediated Endocytosis. *Biochem. J.* **2004**, *377*, 159–169.
10. Sayari, A.; Han, B.-H.; Yang, Y. Simple Synthesis Route to Monodispersed SBA-15 Silica Rods. *J. Am. Chem. Soc.* **2004**, *126*, 14348–14349.
11. Katiyar, A.; Yadav, S.; Smirniotis, P. G.; Pinto, N. G. Synthesis of Ordered Large Pore SBA-15 Spherical Particles for Adsorption of Biomolecules. *J. Chromatogr. A* **2006**, *1122*, 13–20.
12. Qiao, S. Z.; Yu, C. Z.; Hu, Q. H.; Jin, Y. G.; Zhou, X. F.; Zhao, X. S.; Lu, G. Q. Control of Ordered Structure and Morphology of Large-Pore Periodic Mesoporous Organosilicas by Inorganic Salt. *Microporous Mesoporous Mater.* **2006**, *91*, 59–69.
13. Slowing, I.; Trewyn, B. G.; Lin, V. S.-Y. Effect of Surface Functionalization of MCM-41-Type Mesoporous Silica Nanoparticles on the Endocytosis by Human Cancer Cells. *J. Am. Chem. Soc.* **2006**, *128*, 14792–14793.
14. Shen, S.; Chow, P. S.; Chen, F.; Tan, R. B. H. Submicron Particles of SBA-15 Modified with MgO as Carriers for Controlled Drug Delivery. *Chem. Pharm. Bull.* **2007**, *55*, 985–991.
15. Han, Y.; Ying, J. Y. Generalized Fluorocarbon-Surfactant-Mediated Synthesis of Nanoparticles with Various Mesoporous Structures. *Angew. Chem., Int. Ed.* **2005**, *44*, 288–292.
16. Shen, S.; Chen, F.; Chow, P. S.; Phanapavudhikul, P.; Zhu, K.; Tan, R. B. H. Synthesis of SBA-15 Mesoporous Silica *via* Dry-Gel Conversion Route. *Microporous Mesoporous Mater.* **2006**, *92*, 300–308.
17. Zhang, H.; Sun, J.; Ma, D.; Weinberg, G.; Su, D. S.; Bao, X. Engineered Complex Emulsion System: Toward Modulating the Pore Length and Morphological Architecture of Mesoporous Silicas. *J. Phys. Chem. B* **2006**, *110*, 25908–25915.
18. Hoffmann, F.; Cornelius, M.; Morell, J.; Fröba, M. Silica-Based Mesoporous Organic−Inorganic Hybrid Materials. *Angew. Chem., Int. Ed.* **2006**, *45*, 3216–3251.
19. Vallet-Regí, M.; Balas, F.; Arcos, D. Mesoporous Materials for Drug Delivery. *Angew. Chem., Int. Ed.* **2007**, *46*, 7548–7558.
20. Angelos, S.; Liong, M.; Choi, E.; Zink, J. I. Mesoporous Silicate Materials as Substrates for Molecular Machines and Drug Delivery. *Chem. Eng. J.* **2008**, *137*, 4–13.
21. Trewyn, B. G.; Giri, S.; Slowing, I. I.; Lin, V. S. Y. Mesoporous Silica Nanoparticle Based Controlled Release, Drug Delivery, and Biosensor Systems. *Chem. Commun.* **2007**, 3236–3245.
22. Sujandi; Park, S.-E.; Han, D.-S.; Han, S.-C.; Jin, M.-J.; Ohsuna, T. Amino-Functionalized SBA-15 Type Mesoporous Silica Having Nanostructured Hexagonal Platelet Morphology. *Chem. Commun.* **2006**, 4131–4133.
23. Gonzalez, B.; Colilla, M.; Laorden, C. L. d.; Vallet-Regi, M. A Novel Synthetic Strategy for Covalently Bonding Dendrimers to Ordered Mesoporous Silica: Potential Drug Delivery Applications. *J. Mater. Chem.* **2009**, *19*, 9012–9024.
24. Choi, M.; Kleitz, F.; Liu, D.; Lee, H. Y.; Ahn, W.-S.; Ryoo, R. Controlled Polymerization in Mesoporous Silica toward the Design of Organic−Inorganic Composite Nanoporous Materials. *J. Am. Chem. Soc.* **2005**, *127*, 1924–1932.
25. Tian, B.-S.; Yang, C. Temperature-Responsive Nanocomposites Based on Mesoporous SBA-15 Silica and PNIPAAm: Synthesis and Characterization. *J. Phys. Chem. C* **2009**, *113*, 4925–4931.
26. Rosenholm, J. M.; Czuryszkiewicz, T.; Kleitz, F.; Rosenholm, J. B.; Lindén, M. On the Nature of the Brønsted Acidic Groups on Native and Functionalized Mesoporous Siliceous SBA-15 as Studied by Benzylamine Adsorption from Solution. *Langmuir* **2007**, *23*, 4315–4323.
27. Wainer, M.; Marcoux, L.; Kleitz, F. Organic Solvent Treatment and Physicochemical Properties of Nanoporous Polymer-SBA-15 Composite Materials. *J. Mater. Sci.* **2009**, *44*, 6538–6545.
28. Guillet-Nicolas, R.; Marcoux, L.; Kleitz, F. Insights into Pore Surface Modification of Mesoporous Polymer−Silica

Composites: Introduction of Reactive Amines. *New J. Chem.* **2010**, *34*, 355–366.
29. Linton, P.; Alfredsson, V. Growth and Morphology of Mesoporous SBA-15 Particles. *Chem. Mater.* **2008**, *20*, 2878–2880.
30. Amsden, B. Modeling Solute Diffusion in Aqueous Polymer Solutions. *Polymer* **2002**, *43*, 1623–1630.
31. Ng, J. B. S.; Kamali-Zare, P.; Sörensen, M.; Brismar, H.; Hedin, N.; Bergström, L. Intraparticle Transport and Release of Dextran in Silica Spheres with Cylindrical Mesopores. *Langmuir* **2009**, *26*, 466–470.
32. Yiu, H. H. P.; Bruce, I. J. Biological Applications of Organically Functionalised Mesoporous Molecular Sieves and Related Materials. *Stud. Surf. Sci. Catal.* **2003**, *146*, 581–584.
33. Wang, B.; He, T.; Liu, L.; Gao, C. Poly(ethylene glycol) Micropatterns as Environmentally Sensitive Template for Selective or Non-selective Adsorption. *Colloids Surf. B* **2005**, *46*, 169–174.
34. Pohlmeier, A.; Haber-Pohlmeier, S. Ionization of Short Polymethacrylic Acid: Titration, DLS, and Model Calculations. *J. Colloid Interface Sci.* **2004**, *273*, 369–380.
35. Jucker, B. A.; Harms, H.; Hug, S. J.; Zehnder, A. J. B. Adsorption of Bacterial Surface Polysaccharides on Mineral Oxides is Mediated by Hydrogen Bonds. *Colloids Surf. B* **1997**, *9*, 331–343.